J. Electroanal. Chem., 341 (1992) 35–46
Elsevier Sequoia S.A., Lausanne
JEC 02314

Investigation on microelectrodes

Part XVI. Study of the shielding effect at a microband-array electrode

Ju Huangxian, Chen Hongyuan * and Gao Hong (H. Kao)
Department of Chemistry, Nanjing University, Nanjing 210008 (People's Republic of China)

(Received 29 January 1992; in revised form 13 May 1992)

Abstract

Microband electrodes display a very strong edge effect. The diffusion layer at a microband electrode may be considered as a semicylinder. When a microband-array electrode is electrolysed for a long time, these diffusion layers partially overlap each other and the total current is smaller than the sum of the currents at all single-microband electrodes. This is the so-called shielding effect. The degree of shielding can be expressed by a shielding factor S_f which depends on the electrolysis time, the distance between electrodes and the electrode width. A formula to calculate the shielding factor S_f is presented here. The results of theoretical calculations are found to be in good agreement with experimental results reported previously.

INTRODUCTION

There are many remarkable types of behaviour in the field of ultramicroelectrodes [1,2]. The mass transport rate at a microelectrode is greatly enhanced because of non-linear diffusion, which leads to an increase in current density and causes the electrode process to reach the steady state very quickly [1,3]. It is possible to study such electrode processes by means of fast cyclic voltammetry [4,5]. Both microdisk and microband electrodes show a very strong edge effect. The radial term for a microdisk electrode of diameter d is $d/2$, while that for a microband electrode of width W_e is $W_e/2$ [6–8].

In recent years, great progress has been made in the theoretical study of microdisk electrodes [9–11]. The study of microcylinder electrodes is also well developed [12–15]. Several basic studies of microband electrodes have been

* To whom correspondence should be addressed.

directed towards chronoamperometry and linear sweep voltammetry [6,8,16–18]. The application of microband-array electrodes has been reported [19–21]. The steady state chronoamperometric current at interdigitated micro-array electrodes has been studied [22–24], as has overlap of the diffusion layers at a microdisk-array electrode [25]. However, no study on the mass transport at a microband-array electrode and its diffusion current has yet been reported.

In this paper we investigate the diffusion layer at a microband electrode, the overlap of the diffusion layers at a microband-array electrode and its effect on the current, as well as the effect of electrolysis time and electrode constitution on the shielding effect. A formula for calculating the shielding factor S_f is presented. The results of theoretical calculations are found to be in good agreement with experimental results in the literature [19].

THEORY

Diffusion layer at microband-array electrode

For a diffusion layer thickness at an electrode δ, the concentration gradient in the case of the limiting current is c/δ (where c is the bulk concentration of reactant) and the limiting current is

$$I = \frac{nFADc}{\delta} \tag{1}$$

Thus

$$\delta = \frac{nFADc}{I} \tag{2}$$

Besides semi-infinite linear diffusion, the mass transport at an inlaid electrode involves radial diffusion, which is the so-called edge effect. The diffusion current is [7]

$$I = \frac{nFAcD^{1/2}}{(\pi t)^{1/2}} + \frac{nFcDP}{2} = I_{cott} + \frac{nFcDP}{2} \tag{3}$$

which is seen to include an area term A and a perimeter term P.

One type of inlaid electrode is the inlaid band electrode with width W_e and length L. Amatore et al. [26] suggested that the diffusion at a microband electrode is a good approximation to the diffusion at a semicylindrical electrode under quasi-steady-state conditions. Aoki et al. [16] considered that the equiconcentration profiles at a microband electrode approach concentric circles with their centre at the origin as the electrolysis time tends to infinity. Thus the electrode behaviour at long times could be expressed in polar coordinates and they obtained a series of results [16,17]. Using an integral equation method, Coen et al. [8] obtained the result that the diffusion field at a microband electrode approximates to that at a

semicylindrical electrode, and the currents at various times, i.e. $\theta = 4Dt/W_e^2 < 1.8$ and $30 < \theta < 100$, are as follows:

$$I_1 = nFDcA\left(\frac{1}{(D\pi t)^{1/2}} + \frac{1}{W_e}\right) = nFDcW_eL\left(\frac{1}{(D\pi t)^{1/2}} + \frac{1}{W_e}\right) \tag{4}$$

$$I_2 = nFDcL\left(\frac{5.553}{\ln\theta} - \frac{6.791}{(\ln\theta)^2}\right) \tag{5}$$

Aoki et al. [6] obtained a simple approximate (less than 0.8% error) equation for the chronoamperometric *current* at a microband electrode in the domain $\theta' = Dt/W_e^2 < 10^8$, i.e.

$$I_3 = nFDcL\left[(\pi\theta')^{-1/2} + 0.97 - 1.10\exp\left(-\frac{9.90}{|\ln(12.37\theta')|}\right)\right] \tag{6}$$

We can obtain the thicknesses of the diffusion layer at a microband electrode for $\theta < 1.8$, $30 < \theta < 100$ and $\theta' < 10^8$ from eqn. (2) and eqns. (4)–(6) respectively as

$$\delta_1 = \frac{(\pi Dt)^{1/2}W_e}{(\pi Dt)^{1/2} + W_e} \tag{7}$$

$$\delta_2 = \frac{W_e}{5.553/\ln\theta - 6.791/(\ln\theta)^2} \tag{8}$$

$$\delta_3 = \frac{W_e}{(\pi\theta')^{-1/2} + 0.97 - 1.10\exp[-9.9/|\ln(12.37\theta')|]} \tag{9}$$

It is clear that δ at a microband electrode increases with increasing time (shown in Fig. 1) and becomes much smaller in comparison with the Cottrell diffusion layer thickness δ_C because of the edge effect. When t is very short ($\theta < 3 \times 10^{-5}$), both δ_1 and δ_3 tend to $\delta_C = (\pi Dt)^{1/2}$; thus the diffusion is close to semi-infinite linear diffusion. In a system with $D = 7.1 \times 10^{-6}$ cm^2 s^{-1} ($Ru(NH_3)_6^{3+}$ solution) and if $W_e = 2.5 \times 10^{-4}$ cm, then I_1, I_2 and I_3 are applicable for $t < 4 \times 10^{-3}$ s, $0.066 < t < 0.22$ s and $t < 8.8 \times 10^5$ s respectively. In Fig. 1(a), it can be seen that δ_1 can be involved by δ_3 when $t < 4 \times 10^{-3}$ s, while δ_2 can also be involved by δ_3 in the range $0.066 < t < 0.22$ s, therefore δ_3 can be on behalf of the variation in diffusion layer thickness with electrolysis time at a microband electrode.

In contrast to the microdisk electrode, the change in current with electrolysis time at a microband electrode is very small only when t is not too small, and the effect of the electrolysis time can be neglected; thus as the electrode process reaches the quasi-steady state, the voltammetric curves tend to a sigmoidal shape.

When W_e increases, δ increases, and the slopes of the δ vs. W_e curves increase with increasing t (shown in Fig. 2). The smaller W_e is, the larger is the variation in

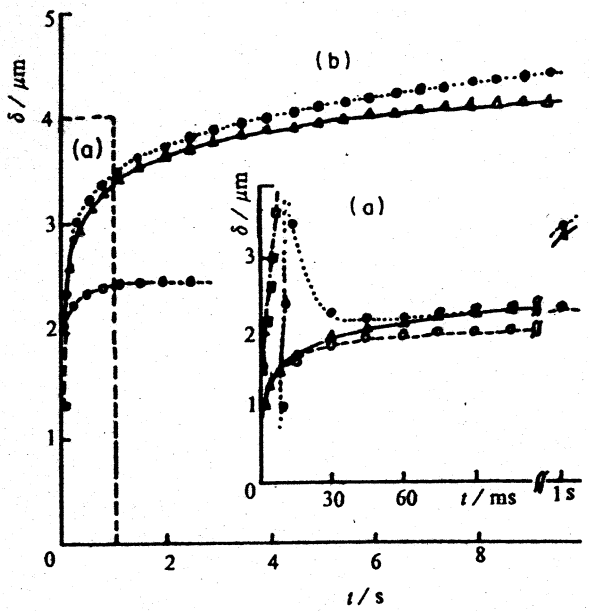

Fig. 1. Theoretical relation between diffusion layer thickness and electrolysis time with $D = 7.1 \times 10^{-6}$ $cm^2\ s^{-1}$ and $W_e = 2.5 \times 10^{-4}$ cm: (a) 0–90 ms; (b) 0–10 s; □, $\delta_C = (\pi Dt)^{1/2}$; ○, eqn. (7); ●, eqn. (8); △, eqn. (9).

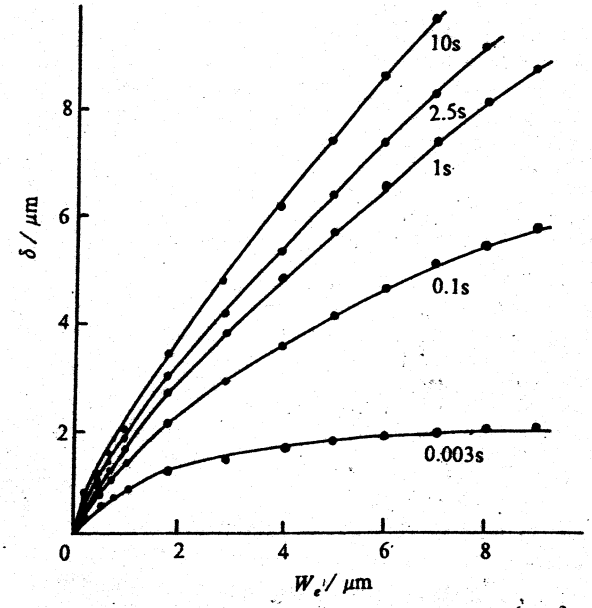

Fig. 2. Relation between δ and W_e with $D = 7.1 \times 10^{-6}$ $cm^2\ s^{-1}$ from eqn. (9).

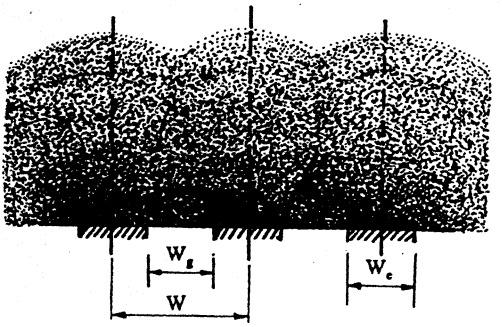

Fig. 3. Diffusion layer model of microband-array electrode.

δ with a change in t and the more easily the electrode process reaches the quasi-steady state.

At a microband-array electrode, if the microband-array electrode involves m microband electrodes, when the electrolysis time is very short ($\theta < 3 \times 10^{-5}$), the mass transport is via plane diffusion and the diffusion layers do not overlap. The total area of all diffusion bands is $S = mW_eL$. With an increase in electrolysis time the edge effect or radial term cannot be neglected and the diffusion layer thickness can be calculated from eqn. (9). If $\delta < W/2$ (W is the central distance between two adjacent electrodes), then the diffusion layers do not overlap and the total interfacial area of all diffusion bands approaches $S = m\pi\delta_3 L$. When $\delta > W/2$, the diffusion layers partially overlap each other and the interfacial area of the diffusion band at the microband-array electrode is smaller than the sum of the areas of all diffusion bands at single electrodes, but the overall electrode process is controlled by diffusion as it is at a single-microband electrode except for the overlap of the diffusion layers. The model is shown in Fig. 3. The maximum diffusion layer thickness can also be expressed by eqn. (9).

Diffusion current at microband-array electrode

The current can be divided into three kinds.

(1) When $\delta < W/2$, the diffusion layers do not overlap and the total current is the sum of the currents at all single-microband electrodes:

$$I = mI_3 \tag{10}$$

where I_3 is given by eqn. (6).

(2) When $\delta > W/2$, the diffusion layers at two adjacent electrodes partially overlap each other. Under this experimental condition the diffusion field approaches a semicylinder. The diffusion band area at a microband-array electrode is

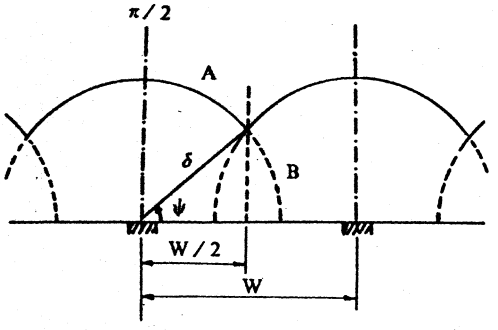

Fig. 4. Cross-sectional model of diffusion layer overlap.

shown in Fig. 4. The diffusion band area at a single microband electrode is AL and

$$A = \pi\delta - 2B, \qquad B = \Psi\delta \tag{11}$$

where

$$\Psi = \tan^{-1}\left(\frac{\left[\delta^2 - (W/2)^2\right]^{1/2}}{W/2}\right) \tag{12}$$

When the electrolysis time increases, both δ and Ψ increase (Ψ can approach $\pi/2$ when the electrolysis time is very large; thus Ψ is in the range 0–$\pi/2$) but the diffusion band area at the microband-array electrode decreases. In Fig. 3, $S = mAL$; thus

$$S = m\left[\pi\delta - 2\delta\tan^{-1}\left(\frac{\left[\delta^2 - (W/2)^2\right]^{1/2}}{W/2}\right)\right]L \tag{13}$$

The total current is expressed as

$$I_{\text{total}} = mnFDcL\left[(\pi\theta')^{-1/2} + 0.97 - 1.10\exp\left(-\frac{9.9}{|\ln(12.37\theta')|}\right)\right]$$
$$\times\left(1 - \left\{2\tan^{-1}\left\{\left[W_c^2/\left\{(\pi\theta')^{-1/2} + 0.97\right.\right.\right.\right.$$
$$\left.\left.\left.\left. - 1.10\exp[-9.9/|\ln(12.37\theta')|]\right\}^2 - (W/2)^2\right]^{1/2}/(W/2)\right\}\right\}(\pi)^{-1}\right) \tag{14}$$

This is lower than the sum of the currents at all single-microband electrodes. Equation (14) was derived from eqn. (6); thus it is valid if $\theta < 10^8$ under the conditions that the mass transfer process can be expressed as a time-dependent two-dimensional diffusion, the microband electrode is so long that the edge effect at both ends is negligible and $\delta > W/2$.

(3) In the limiting situation $\Psi \to \pi/2$ the diffusion layers completely overlap. The electrode can be treated as a plane semi-infinite diffusion electrode with width mW and length L. The current is

$$I = \frac{nFcDm(W_e + W_g)L}{(\pi Dt)^{1/2}} \tag{15}$$

where W_g is the edge distance of two adjacent electrodes.

Shielding effect at microband-array electrode

In the electrolysis process the electrodes shield each other because of the overlap of diffusion bands; thus the current is reduced. This is the so-called "shielding effect". The degree of shielding can be expressed by the shielding factor

$$S_f = 1 - \frac{I_{total}}{\sum_{j=1}^{m} I_j} \tag{16}$$

where I_j is the current of the jth electrode only when this electrode is electrolysed with all other electrodes in open circuit. Obviously, the shielding factor represents the ratio of the area of the diffusion band overlapped at the microband-array electrode to the total area of the diffusion bands at all single electrodes. If the microband-array electrode involves m ($m \to \infty$) microband electrodes, then the shielding factor is

$$S_f = \frac{2\Psi}{\pi} \tag{17}$$

or

$$S_f = \left(2\tan^{-1}\left\{\left[W_e^2/\left\{(\pi\theta')^{-1/2} + 0.97 - 1.10\exp[-9.9/|\ln(12.37\theta')|]\right\}^2 - (W/2)^2\right]^{1/2}/(W/2)\right\}\right)(\pi)^{-1} \tag{18}$$

Thus the shielding effect depends on the electrolysis time and the electrode constitution.

DISCUSSION

Dependence of current I_{total} at microband-array electrode on electrolysis time t and electrode width W_e

It can be concluded from the comparison between eqns. (6) and (14) that the current I_{total} at a microband-array electrode is much smaller than the sum of the

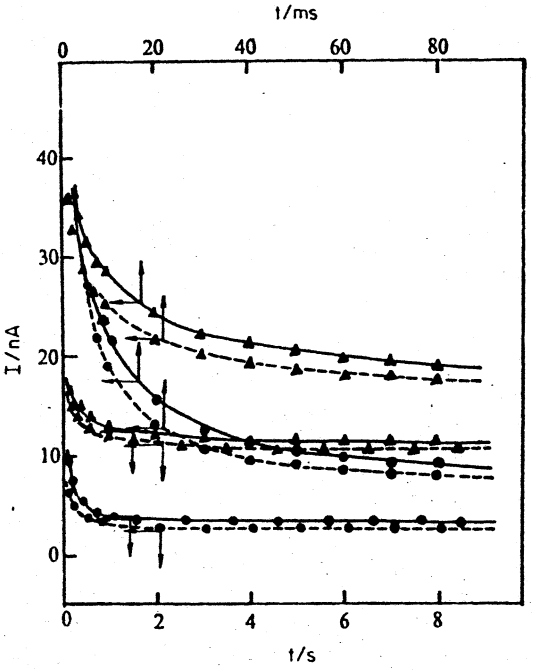

Fig. 5. Dependence of current at microband-array electrode on t with $D = 7.1 \times 10^{-6}$ cm^2 s^{-1}: ●, with shielding effect; ▲, without shielding effect; — — —, $W_e = 2.5$ μm, $W_g = 1$ μm; ———, $W_e = 3.3$ μm, $W_g = 0.2$ μm.

currents at all single-microband electrodes. When W_g is fixed, the difference between the two currents increases with increasing t and tends to a steady value (see Fig. 5). If all other conditions are fixed, I_{total} falls very quickly as W_g is reduced. In Fig. 6, the larger W_e is, the larger is the total current and the variation in I_{total} with W_e has a minimum value. All these factors affect the overlap of the diffusion layers and the shielding effect.

Dependence of shielding effect on t, W_e and W_g

From eqn. (18), S_f increases with increasing t and tends to a steady value quickly (see Fig. 7(a)). The larger the ratio W_e/W_g is, the larger is S_f. When W_g is fixed, the variation in S_f with W_e has a maximum value. When W_e is very small, S_f tends to zero (see Fig. 7(b)). When W_g increases, S_f falls and tends quickly to zero. The smaller the value of W_g is, the smaller is t when $S_f = 0$ (see Fig. 8).

Comparison with experimental results

In any controlled potential experiment conducted with a large value of θ, i.e. under the condition of a quasi-steady state, the limiting current under the diffu-

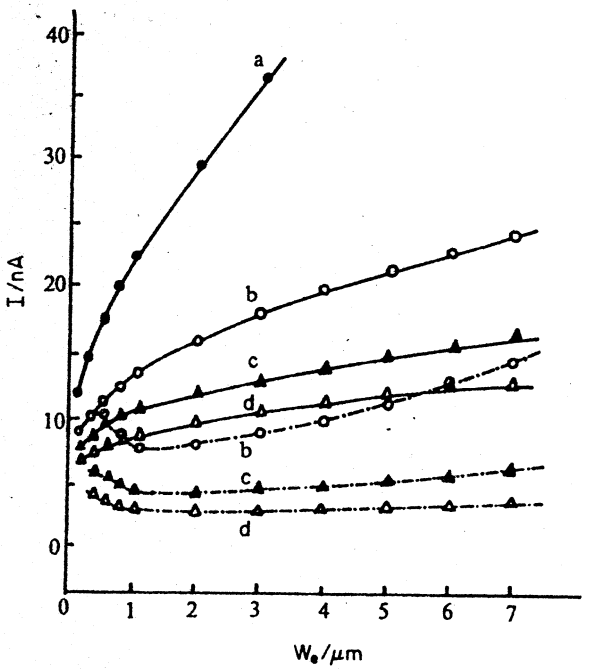

Fig. 6. Dependence of current at microband-array electrode on W_c: a, 0.003 s; b, 0.1 s; c, 1 s; d, 10 s; other conditions as Fig. 5.

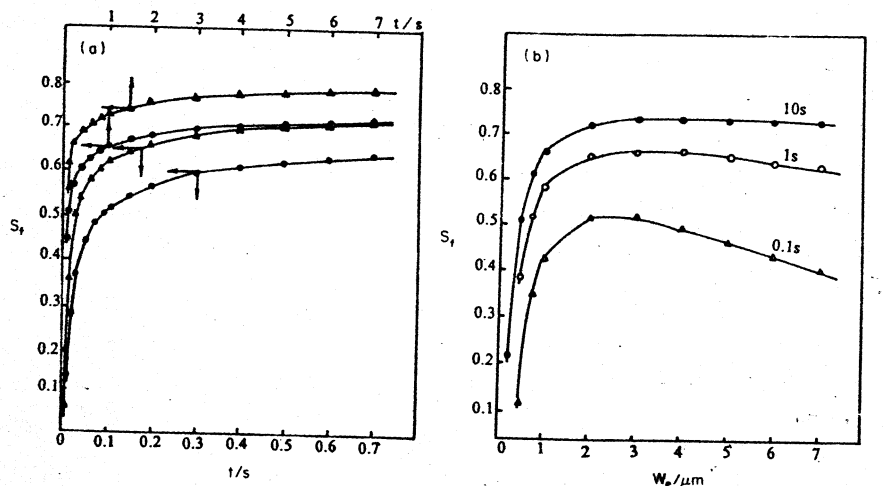

Fig. 7. Dependence of S_f on (a) t and (b) W_c with $D = 7.1 \times 10^{-6}$ cm^2 s^{-1}: (a) ○, $W_g = 1$ μm, $W_e = 2.5$ μm; △, $W_g = 0.2$ μm, $W_e = 3.3$ μm; (b) $W_g = 1$ μm.

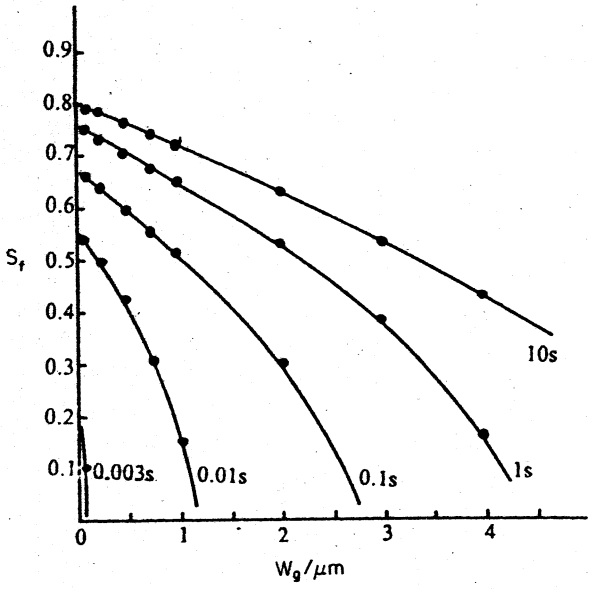

Fig. 8. Relation between S_f and W_g with $D = 7.1 \times 10^{-6}$ cm^2 s^{-1} and $W_e = 2.5$ μm.

sion-controlled condition will be the same [27] whatever the potential excitation. For example, with cyclic voltammetry at a sufficiently slow rate, the limiting current may be calculated by means of the chronoamperometric current equation [8,19,20] and the real experimental time or characteristic time is [20]

$$t = \frac{RT}{Fv} \tag{19}$$

where v is the scan rate. Results in the literature [19,20,22] indicate that the theoretical currents obtained from the chronoamperometric current equation with the usual electrolysis times are in keeping with the cyclic voltammetric experimental currents in the case of slow scan rates. The theoretical current and the shielding factor for a microband-array electrode can be obtained from eqns. (19), (14) and (18). It must be considered that only one side of the diffusion layers at the two outside electrodes is able to overlap. Thus for a finite value of m the shielding factor is

$$S_{\text{ftotal}} = \frac{(m-1)S_f}{m} \tag{20}$$

In Table 1 we list the theoretically calculated shielding factors of microband-array electrodes involving different m values with $W_e = 2.5$ μm and $W_g = 1$ μm and compare them with results calculated from literature data [19].

It can be seen that at array electrodes composed of two, three, four or eight microbands the values calculated theoretically by eqn. (18) are very close to those

TABLE 1

Comparison of literature experimental values of shielding factor with theoretical values in this paper [a]

	$m = 2$	$m = 3$	$m = 4$	$m = 8$	$m = 12$
Distance between adjacent electrodes/μm	1.0	1.0	1.0	1.0	22
S_f' theoretical value [b]	0.35	0.47	0.53	0.62	0
$(S_f)_l$ experimental results [c]	0.39	0.54	0.56	0.72	0.11
$(S_f)_l - S_f'$	0.04	0.07	0.03	0.10	0.11

[a] $D = 7.1 \times 10^{-6}$ cm^2 s^{-1}, $W_c = 2.5$ μm, $W_g = 1.0$ μm, $v = 10$ mV s^{-1}, $t = 2.5$ s.
[b] Obtained from eqn. (18).
[c] Using literature data [19] in eqn. (16).

obtained from the literature experimental data [19] by eqn. (16), and the relative error is very small. At an array electrode consisting of two microbands with $W_g = 22$ μm the shielding factor should be very small; the theoretically calculated value is zero, but the value from the experimental data is 0.11. This discrepancy can be explained as follows. When the working electrode was swept with a cyclic potential, the potential of adjacent electrodes was zero. This reduced the measured current and resulted in a reduction in the collection efficiency by about 7%–10% [19]. Thus all the shielding factors obtained from experiments were higher than those obtained by theoretical calculations. The values of $(S_f)_l - S_f'$ were in the range 0.03–0.11, which suggests that if the factor of collection efficiency were corrected, the theoretical values would be in much better agreement with the experimental values.

ACKNOWLEDGEMENT

This project was supported by the National Natural Science Foundation of China.

REFERENCES

1 R.M. Wightman, Anal. Chem., 53 (1981) 1125A.
2 T. Hepel and J. Osteryoung, J. Phys. Chem., 86 (1982) 1406.
3 Ju Huangxian and Chen Hongyuan, Chem. Sensors (Chinese), 10(1) (1990) 1.
4 J.O. Howell and R.M. Wightman, J. Phys. Chem., 88 (1984) 3915.
5 M.I. Montenegro and D. Pletcher, J. Electroanal. Chem., 200 (1986) 371.
6 K. Aoki, K. Tokuda and H. Matsuda, J. Electroanal. Chem., 230 (1987) 61.
7 K.B. Oldham, J. Electroanal. Chem., 122 (1981) 1.
8 S. Coen, D.K. Cope and D.E. Tallman, J. Electroanal. Chem., 215 (1986) 29.
9 K. Aoki, K. Tokuda and H. Matsuda, J. Electroanal. Chem., 235 (1987) 87.
10 A.M. Bond, K.B. Oldham and C.G. Zoski, J. Electroanal. Chem., 245 (1988) 71.
11 C.G. Zoski, A.M. Bond, E.T. Allinson and K.B. Oldham, Anal. Chem., 62 (1990) 37.
12 K. Aoki, K. Honda, K. Tokuda and H. Matsuda, J. Electroanal. Chem., 186 (1985) 79.
13 C.A. Amatore, M.R. Deakin and R.M. Wightman, J. Electroanal. Chem., 206 (1986) 23.
14 K. Aoki, K. Honda, K. Tokuda and H. Matsuda, J. Electroanal. Chem., 199 (1986) 271.
15 K. Aoki, K. Tokuda and H. Matsuda, J. Electroanal. Chem., 206 (1986) 47.

16 K. Aoki, K. Tokuda and H. Matsuda, J. Electroanal. Chem., 225 (1987) 19.
17 K. Aoki and K. Tokuda, J. Electroanal. Chem., 237 (1987) 163.
18 A. Szabo, D.K. Cope, D.E. Tallman, P.M. Kovach and R.M Wightman, J. Electroanal. Chem., 217 (1987) 417.
19 A.J. Bard, J.A. Crayston, G.P. Kittllesen, T.V. Shoa and M.S. Wighton, Anal. Chem., 58 (1986) 2321.
20 T.V. Shea and A.J. Bard, Anal. Chem., 59 (1987) 2101.
21 E.W. Paul, A.J. Ricco and M.S. Wrighton, J. Phys. Chem., 89 (1985) 1441.
22 H. Allen, H.O. Hall, N.A. Klein, I.S.M. Psalti and N.J. Walton, Anal. Chem., 61 (1989) 2200.
23 K. Aoki, J. Electroanal. Chem., 270 (1989) 35.
24 K. Aoki and M. Tanaka, J. Electroanal. Chem., 266 (1989) 11.
25 B.R. Scharifker, J. Electroanal. Chem., 240 (1988) 61.
26 C.A. Amatore, B. Fosset, M.R. Deakin and R.M. Wightman, J. Electroanal. Chem., 225 (1987) 33.
27 R.M. Wightman and D.O. Wipf, in A.J. Bard (Ed.), Electroanalytical Chemistry, Vol. 15, Marcel Dekker, New York, 1989, pp. 270, 276, 285–289, 295.